J. Phys.: Condens. Matter **21** (2009) 215602 (11pp) doi:10.1088/0953-8984/21/21/215602

Spin fluctuation effects on the conductance through a single Pd atom contact

M A Romero[1], S C Gómez-Carrillo[2], P G Bolcatto[2,3] and E C Goldberg[1,4]

[1] Instituto de Desarrollo Tecnológico para la Industria Química (INTEC), Universidad Nacional del Litoral, Consejo Nacional de Investigaciones Científicas y Técnicas (CONICET), Güemes 3450 CC 91, 3000 Santa Fe, Argentina
[2] Departamento de Física, Facultad de Ingeniería Química, Universidad Nacional de Litoral, Santiago del Estero 2829, 3000 Santa Fe, Argentina
[3] Facultad de Humanidades y Ciencias, Universidad Nacional del Litoral, Argentina
[4] Departamento de Materiales, Facultad de Ingeniería Química, Universidad Nacional del Litoral, 3000 Santa Fe, Argentina

Received 11 November 2008, in final form 9 March 2009
Published 24 April 2009
Online at stacks.iop.org/JPhysCM/21/215602

Abstract
A controversy about the conductance through single atoms still exists. There are many experiments where values lower than the quantum unity $G_0 = 2e^2/h$ have been found associated to Kondo regimes with high Kondo temperatures. Specifically in the Pd single atom contact, conductance values close to $G_0/2$ at room temperature have been reported. In this work we propose a theoretical analysis of a break junction of Pd where the charge fluctuation in the single atom contact is limited to the most probable one: $d^{10} \leftrightarrow d^9$. The projected density of states and the characteristics of the electron transport are calculated by using a realistic description of the interacting system. A Kondo regime is found where the conductance values and their dependence on temperature are in good agreement with the experimental trends observed in the conduction of single molecule transistors based on transition metal coordination complexes.

(Some figures in this article are in colour only in the electronic version)

1. Introduction

Atomic sized contacts have been made possible through techniques such as controllable break junctions and scanning tunneling microscopy, and the properties of such atomic contacts have been studied for many different magnetic and nonmagnetic metals [1]. In the ballistic regime the conductance of these junctions is described by the Landauer formula,

$$G = G_0 \sum_i T_i \tag{1}$$

where the summation is extended to all the available channels traversing the atom contact; T_i is a number between 0 and 1 for the transmission of the ith-channel, and $G_0 = 2e^2/h$ is the quantum conductance assuming spin degeneracy, e being the elemental charge and h Planck's constant. In the case in which the degeneracy is removed, the channels have to be redefined for each spin and each of these carries up to $G_0/2$. Also when the conductance is dominated by a single orbital channel and a strong Coulomb interaction completely blocks transport through one of the spin subchannel, it is expected that there will be a conductance value close to a half of G_0.

Several claims of the observation of half-integer conductance quantization for both magnetic and nonmagnetic metals have appeared [2–5], but there are also many works that contradict these observations [6–8]. As has been largely discussed in the literature, the number of channels available in a one atom contact is determined by the valence of the metal, and the transmission of each channel is influenced by parameters such as the number of neighbors, the bond distance, and the symmetry of the valence orbitals [9–11]. For s-type metals such as Au the electronic transport through a single atom will be due to a single channel with a transmission close to unity, but this is not the case for transition metals with partial occupation of d-orbitals, where the combinations of all channels with different transmissions will contribute to determine a conductance equal to some fractional number of G_0.

 © 2009 IOP Publishing Ltd Printed in the UK

In this work we will analyze atomic sized contacts of Pd. There is experimental evidence showing that Pd breaks essentially at the level of a single atom [5, 12], but up to now there seems to be a controversy about the characteristic conductance of a Pd single atom contact (SAC). Rodrigues *et al* [5] claim to have measured a half quantization of the conductance at room temperature, compatible with a fully polarized conduction channel, while other authors report a conductance smaller than one and close to $G_0/2$ only when the contact is exposed to gas molecules [6, 8]. On the other hand, experiments based on scanning tunneling spectroscopy have detected Kondo resonances with large Kondo temperatures in metal transition atoms adsorbed in metal surfaces [13, 14], and in the conduction of single-molecule transistors based on transition metal coordination complexes [15, 16]. In the first case it has also been reported that there is a pronounced dependence of the Kondo resonance with the d-shell occupancy of the transition metal adsorbate in such a way that it is largest for atoms near to the ends of the 3d row. The question is, can Pd SAC present Kondo resonance features in some appropriate break junction process? We propose in this work a theoretical situation based on a break junction geometry not far from the reality [5, 12], and where the most probable d^{10}–d^9 charge transition is considered in the Pd SAC in the case of low values of the applied bias potential. A model Hamiltonian is proposed that includes the conductance channels according to a strong correlation effect that limits the charge fluctuation to only one electron, and the Keldysh Green functions are used for calculating the electron transport process [17]. The projected local density of states on the Pd atom between the two Pd surface contacts, and the characteristics of the electron transport when a bias voltage is applied, are calculated by using a realistic description of the electronic structure of the Pd leads and of the atom-lead interaction parameters.

2. Theory

The interacting system is shown in figure 1. We identify three subsystems: the left lead (L), the SAC and the right lead (R) (see the inset). The two leads are assumed to be pyramidal structures grown in the [100] direction. The local density of states (LDOS) on the outermost atom of each lead is shown in figure 1. It was calculated by using the Fireball code [18] which is an *ab initio* local density approximation (LDA)-based approximation to the electronic problem. In this figure the energy level of a hole is also indicated, added to the zero hole configuration of the Pd central atom (d^{10}–d^9 electronic transition). The d-orbitals are assumed degenerated by neglecting the crystalline field effect.

2.1. Model Hamiltonian

The Hamiltonian includes the following five terms:

$$H = H_{\mathrm{L}} + H_{\mathrm{R}} + H_{\mathrm{SAC}} + H_{\mathrm{L-SAC}} + H_{\mathrm{R-SAC}} \qquad (2)$$

where $H_{\mathrm{L(R)}} = \sum_{\mathrm{k},\sigma} \epsilon_{\mathrm{kL(R)}} \hat{n}_{\mathrm{kL(R)},\sigma}$ corresponds to the non-perturbed states of the contact surfaces with energy $\epsilon_{\mathrm{kL(R)}}$ and occupation number operator $\hat{n}_{\mathrm{kL(R)},\sigma} = \hat{c}^{+}_{\mathrm{kL(R)},\sigma} \hat{c}_{\mathrm{kL(R)},\sigma}$.

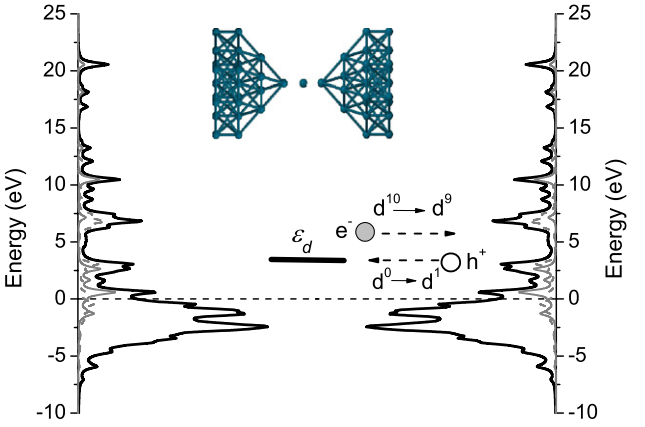

Figure 1. Local density of states on the end atom of the tip. The sum of the diagonal terms (black solid line) and the sum of p (gray solid line) and s (gray dashed line) band states are shown. A scheme of the device is also indicated and the hole (electron) transition process used in our proposal.

The electrons in the leads are assumed to be noninteracting except for an overall self-consistent potential, by considering the typical experimental geometry in which the leads rapidly broaden into metallic contacts. The occupation, for each contact, is determined by an equilibrium distribution function established before the tunneling matrix elements are turned on [19]. It is assumed that the leads interact only through the Pd SAC.

The Pd single atom electronic configurations according to the considered most probable d^{10}–d^9 charge fluctuation are written by using a hole description in which we deal with the d^0–d^1 transition (see figure 1). In this hole picture, and considering the five-fold degeneration of d-orbitals, we have the following states $|S, M\rangle$ classified by the total spin S and its projection M:

$$\mathrm{d}^0 \Rightarrow |0,0\rangle = |00000\rangle \text{ (zero hole)} \qquad (3)$$

$$\mathrm{d}^1 \Rightarrow |1/2,\sigma\rangle = \frac{1}{\sqrt{5}}[|\sigma 0000\rangle + |0\sigma 000\rangle + |00\sigma 00\rangle + |000\sigma 0\rangle + |0000\sigma\rangle] \text{ (one hole)} \qquad (4)$$

and where σ can be either $1/2$ or $-1/2$. By using the projection operators [20] for these selected atomic configurations we can write:

$$H_{\mathrm{SAC}} = \varepsilon_0 |0,0\rangle\langle 0,0| + \sum_{\sigma} \varepsilon_{1/2} |1/2,\sigma\rangle\langle 1/2,\sigma|. \qquad (5)$$

In the present case the considered Pd charge configurations correspond to either a neutral atom or positive ion Pd^{+}. We are assuming that the Pd^{++} ion configuration will be much less probable for not very large values of the bias potential, because of the low $E(\mathrm{d}^9) - E(\mathrm{d}^8)$ energy value relative to the Fermi level of the leads. This means, in the hole picture, two strongly correlated degenerated spin states restricted to a single occupation. Nevertheless in this particular case the same results can be obtained by using a slave-boson approach to the Anderson model [21], the projection operator technique allows us to select in a clear way all the atomic configurations involved in more complex problems related with charge and spin

fluctuations [22]. The interaction terms, consistently with the Anderson model $H_{\alpha-\mathrm{SAC}} = \sum_{\mathrm{k},\sigma,\mathrm{d}}[V_{\mathrm{k}\alpha,\mathrm{d}}\hat{c}^{+}_{\mathrm{k}\alpha,\sigma}\hat{c}_{\mathrm{d},\sigma} + \mathrm{c.c}]$, are constructed by taking into account that:

$$\sum_{\mathrm{k},\sigma,\mathrm{d}} V_{\mathrm{k}\alpha,\mathrm{d}}\hat{c}^{+}_{\mathrm{k}\alpha,\sigma}\hat{c}_{\mathrm{d},\sigma}|1/2,\sigma\rangle = \sum_{\mathrm{k},\sigma}\tilde{V}_{\mathrm{k}\alpha}\hat{c}^{+}_{\mathrm{k}\alpha,\sigma}|0,0\rangle \quad \text{with } \alpha = \mathrm{L},\mathrm{R} \tag{6}$$

where $\tilde{V}_{\mathrm{k}\alpha} = 1/\sqrt{5}\sum_{\mathrm{d}=1-5} V_{\mathrm{k}\alpha,\mathrm{d}}$ has been defined, $V_{\mathrm{k}\alpha,\mathrm{d}}$ being the hopping term between the d-orbitals of the Pd SAC and the k-band states of the lead (α). According to equation (6), the interaction term can be written as:

$$H_{\alpha-\mathrm{SAC}} = \sum_{\mathrm{k},\sigma}[\tilde{V}_{\mathrm{k}\alpha}\hat{c}^{+}_{\mathrm{k}\alpha,\sigma}|0,0\rangle\langle 1/2,\sigma| + \mathrm{c.c.}]. \tag{7}$$

2.2. Green functions. Equations of motion

The following two Green functions are required for solving a general non-equilibrium process [17]:

$$G_\sigma(t,t') = \mathrm{i}\Theta(t'-t)\langle\Phi_0|\{|1/2,\sigma\rangle\langle 0,0|_{t'}, |0,0\rangle\langle 1/2,\sigma|_t\} \times |\Phi_0\rangle \tag{8}$$

$$F_\sigma(t,t') = \mathrm{i}\langle\Phi_0|[|1/2,\sigma\rangle\langle 0,0|_{t'}, |0,0\rangle\langle 1/2,\sigma|_t]|\Phi_0\rangle \tag{9}$$

where {} and [ ] indicate anticommutator and commutator respectively; and Φ_0 is the wavefunction of the interacting system in the Heisenberg representation. These Green functions are calculated by employing the method of equations of motion (EOM) closed up to a second order in the atom-surface coupling parameter $V_{\mathrm{k}\alpha}$. This calculation provides a very accurate description of non-equilibrium processes when the motion equations are closed within a strict second order in $V_{\mathrm{k}\alpha}$ [21–24]. It is interesting to see in some detail the EOM method applied for *both* Green functions written in terms of the projector operators used to describe the hole states of the Pd SAC:

2.2.1. Calculation of $G_\sigma(t,t')$. The time derivative of the Green function $G_\sigma(t,t')$ is determined by the explicit terms of the Hamiltonian given by equation (2) (atomic units are used unless stated otherwise):

$$\begin{aligned}\mathrm{i}\frac{\mathrm{d}G_\sigma(t,t')}{\mathrm{d}t} &= \delta(t-t')\langle\Phi_0|1/2,\sigma\rangle\langle 1/2,\sigma| \\ &+ |0,0\rangle\langle 0,0|\Phi_0\rangle + (\varepsilon_{1/2}-\varepsilon_0)G_\sigma(t,t') \\ &+ \sum_{\mathrm{k}\alpha}\tilde{V}^{*}_{\mathrm{k}\alpha}G_\sigma(|0,0\rangle\langle 0,0|\hat{c}_{\mathrm{k}\alpha,\sigma}) \\ &+ \sum_{\mathrm{k}\alpha}\tilde{V}^{*}_{\mathrm{k}\alpha}G_\sigma(|1/2,\sigma\rangle\langle 1/2,\sigma|\hat{c}_{\mathrm{k}\alpha,\sigma}) \\ &+ \sum_{\mathrm{k}\alpha}\tilde{V}^{*}_{\mathrm{k}\alpha}G_\sigma(|1/2,-\sigma\rangle\langle 1/2,\sigma|\hat{c}_{\mathrm{k}\alpha,-\sigma})\end{aligned} \tag{10}$$

where the following notation has been used for the new Green functions appearing in equation (10):

$$G_\sigma\big(|A\rangle\langle B|\hat{c}_{\mathrm{k}\alpha,\sigma}\big) = \mathrm{i}\Theta(t'-t)\langle\Phi_0|\{|1/2,\sigma\rangle \times \langle 0,0|_{t'}, |A\rangle\langle B|\hat{c}_{\mathrm{k}\alpha,\sigma}(t)\}|\Phi_0\rangle. \tag{11}$$

By taking the time derivatives of these new Green functions and closing up to a second order in $\tilde{V}_{\mathrm{k}\alpha}$, the following equations are obtained:

$$\begin{aligned}\mathrm{i}\frac{\mathrm{d}G_\sigma\big(|0,0\rangle\langle 0,0|\hat{c}_{\mathrm{k}\alpha,\sigma}\big)}{\mathrm{d}t} &= \delta(t-t')\langle\Phi_0|1/2,\sigma\rangle \\ &\times \langle 0,0|\hat{c}_{\mathrm{k}\alpha,\sigma}|\Phi_0\rangle + \epsilon_{\mathrm{k}\alpha}G_\sigma(|0,0\rangle\langle 0,0|\hat{c}_{\mathrm{k}\alpha,\sigma}) \\ &+ \tilde{V}_{\mathrm{k}\alpha}\langle 1-\hat{n}_{\mathrm{k}\alpha,\sigma}\rangle G_\sigma(t,t')\end{aligned} \tag{12}$$

$$\begin{aligned}\mathrm{i}\frac{\mathrm{d}G_\sigma\big(|1/2,\sigma\rangle\langle 1/2,\sigma|\hat{c}_{\mathrm{k}\alpha,\sigma}\big)}{\mathrm{d}t} &= -\delta(t-t')\langle\Phi_0|1/2,\sigma\rangle \\ &\times \langle 0,0|\hat{c}_{\mathrm{k}\alpha,\sigma}|\Phi_0\rangle \\ &+ \epsilon_{\mathrm{k}\alpha}G_\sigma(|1/2,\sigma\rangle\langle 1/2,\sigma|\hat{c}_{\mathrm{k}\alpha,\sigma}) \\ &+ \tilde{V}_{\mathrm{k}\alpha}\langle\hat{n}_{\mathrm{k}\alpha,\sigma}\rangle G_\sigma(t,t')\end{aligned} \tag{13}$$

$$\begin{aligned}\mathrm{i}\frac{\mathrm{d}G_\sigma(|1/2,-\sigma\rangle\langle 1/2,\sigma|\hat{c}_{\mathrm{k}\alpha,-\sigma})}{\mathrm{d}t} &= -\delta(t-t')\langle\Phi_0|1/2,-\sigma\rangle \\ &\times \langle 0,0|\hat{c}_{\mathrm{k}\alpha,-\sigma}|\Phi_0\rangle \\ &+ \epsilon_{\mathrm{k}\alpha}G_\sigma(|1/2,-\sigma\rangle\langle 1/2,\sigma|\hat{c}_{\mathrm{k}\alpha,-\sigma}) \\ &+ \tilde{V}_{\mathrm{k}\alpha}\langle\hat{n}_{\mathrm{k}\alpha,-\sigma}\rangle G_\sigma(t,t').\end{aligned} \tag{14}$$

In the case of stationary processes ($\tilde{V}_{\mathrm{k}\alpha}$ does not depend on time), by Fourier transforming equations (12)–(14), and replacing them in the Fourier transform of equation (10), we arrive at the final expression:

$$\begin{aligned}&\left\{\omega - (\varepsilon_{1/2}-\varepsilon_0) - \sum_{\mathrm{k}\alpha}\frac{|\tilde{V}_{\mathrm{k}\alpha}|^2}{\omega-\epsilon_{\mathrm{k}\alpha}-\mathrm{i}\eta}\right. \\ &\left. - \sum_{\mathrm{k}\alpha}\frac{|\tilde{V}_{\mathrm{k}\alpha}|^2\langle\hat{n}_{\mathrm{k}\alpha,-\sigma}\rangle}{\omega-\epsilon_{\mathrm{k}\alpha}-\mathrm{i}\eta}\right\}G_\sigma(\omega) \\ &= \langle\Phi_0|1/2,\sigma\rangle\langle 1/2,\sigma| + |0,0\rangle\langle 0,0|\Phi_0\rangle \\ &+ \sum_{\mathrm{k}\alpha}\frac{\tilde{V}^{*}_{\mathrm{k}\alpha}\langle\Phi_0|1/2,-\sigma\rangle\langle 0|\hat{c}_{\mathrm{k}\alpha,-\sigma}|\Phi_0\rangle}{\omega-\epsilon_{\mathrm{k}\alpha}-\mathrm{i}\eta}\end{aligned} \tag{15}$$

where $\langle\hat{n}_{\mathrm{k}\alpha,-\sigma}\rangle = f^{\mathrm{FD}}(\epsilon_{\mathrm{k}\alpha})$ is the Fermi–Dirac distribution (of holes in this case) given by:

$$\begin{aligned}f^{\mathrm{FD}}(\epsilon_{\mathrm{k}\alpha}) &= 1 - 1/[1+\exp((\epsilon_{\mathrm{k}\alpha}-\mu_\alpha)/k_{\mathrm{B}}T)] \\ &= 1/[1+\exp(-(\epsilon_{\mathrm{k}\alpha}-\mu_\alpha)/k_{\mathrm{B}}T)],\end{aligned} \tag{16}$$

where μ_α is the Fermi energy of the contact surface (α). This is the main difference with the decoupling approach proposed by Lacroix [23], where mean values $\langle\hat{c}^{+}_{\mathrm{k}\alpha,\sigma}\hat{c}_{\mathrm{k}\alpha,\sigma}\rangle$ are also recalculated, leading to a non-consistent second order solution [21]. In the case of the decoupling schemes of Meir *et al* [25], the correlation functions $\langle\Phi_0|1/2,-\sigma\rangle\langle 0,0|\hat{c}_{\mathrm{k}\alpha,\sigma}|\Phi_0\rangle$ that appear in equations (12)–(14) are neglected, this being a good approximation only for large values of the temperature.

The equation (15) is solved by taking into account the norm constraint:

$$\sum_\sigma\langle\Phi_0|1/2,\sigma\rangle\langle 1/2,\sigma|\Phi_0\rangle + \langle\Phi_0|0,0\rangle\langle 0,0|\Phi_0\rangle = 1. \tag{17}$$

2.2.2. Calculation of $F_\sigma(t,t')$. The equations of motion of $F_\sigma(t,t')$ are obtained by following a completely analogous procedure as for $G_\sigma(t,t')$. But in this case we need to use the boundary conditions given by:

$$\begin{aligned}F_\sigma\big(|A\rangle\langle B|\hat{c}_{\mathrm{k}\alpha,\sigma}(-\infty)\big) &= \mathrm{i}\langle\Phi_0|[|1/2,\sigma\rangle\langle 0,0|_{t'}, |A\rangle \\ &\times \langle B|\hat{c}_{\mathrm{k}\alpha,\sigma}(-\infty)]|\Phi_0\rangle \\ &= [2\langle\hat{n}_{\mathrm{k}\alpha,\sigma}\rangle - 1]G_\sigma(|A\rangle\langle B|\hat{c}_{\mathrm{k}\alpha,\sigma}(-\infty))\end{aligned} \tag{18}$$

for arriving at the final expression:

$$\begin{aligned}&\left\{\omega-(\varepsilon_{1/2}-\varepsilon_0)-\sum_{k\alpha}\frac{|\tilde{V}_{k\alpha}|^2}{\omega-\epsilon_{k\alpha}+i\eta}\right.\\&\quad\left.-\sum_{k\alpha}\frac{|\tilde{V}_{k\alpha}|^2\langle\hat{n}_{k\alpha,-\sigma}\rangle}{\omega-\epsilon_{k\alpha}+i\eta}\right\}F_\sigma(\omega)\\&=-2\pi i\sum_{k\alpha}\tilde{V}^*_{k\alpha}\left[2\langle\hat{n}_{k\alpha,-\sigma}\rangle-1\right]\langle\Phi_0|1/2,-\sigma\rangle\\&\quad\times\langle 0|\hat{c}_{k\alpha,-\sigma}|\Phi_0\rangle\delta(\omega-\epsilon_{k\alpha})\\&\quad+2\pi i\sum_{k\alpha}\left|\tilde{V}_{k\alpha}\right|^2[2\langle\hat{n}_{k\alpha,\sigma}\rangle-1][\langle\hat{n}_{k\alpha,-\sigma}\rangle+1]\\&\quad\times\delta(\omega-\epsilon_{k\alpha})G_\sigma(\omega).\end{aligned}\tag{19}$$

In the case of *equilibrium processes*, the Green function $G_\sigma(\omega)$ is the only one necessary for calculating the SAC properties. In this case, the projected density of states on the single atom interacting with the leads,

$$\rho_\sigma(\omega)=\frac{1}{\pi}\,\mathrm{Im}\,G_\sigma(\omega)\tag{20}$$

the hole-state occupation per spin,

$$\langle n_\sigma\rangle=\langle\Phi_0|1/2,\sigma\rangle\langle 1/2,\sigma|\Phi_0\rangle=\int d\omega\, f^{FD}(\omega)\rho_\sigma(\omega),\tag{21}$$

and the correlation function,

$$\begin{aligned}&\langle\Phi_0|1/2,-\sigma\rangle\langle 0,0|\hat{c}_{k\alpha,-\sigma}|\Phi_0\rangle\\&=\tilde{V}_{k\alpha}\int d\omega\, f^{FD}(\omega)\,\mathrm{Im}\,\frac{G_{-\sigma}(\omega)}{\omega-\epsilon_{k\alpha}-i\eta}\end{aligned}\tag{22}$$

are all derived from the knowledge of $G_\sigma(\omega)$.

While in the general case of *non-equilibrium stationary processes* both $G_\sigma(\omega)$ and $F_\sigma(\omega)$ are required for calculating the different correlation functions in the following way (spin degeneration is being considered):

$$\begin{aligned}\langle n_\sigma\rangle&=\frac{1-iF_\sigma(t,t)}{3}=\frac{1}{3}\left[1-\frac{i}{2\pi}\int_{-\infty}^{\infty}d\omega\,F_\sigma(\omega)\right]\\&=\frac{1}{4\pi i}\int_{-\infty}^{\infty}d\omega\,[F_\sigma(\omega)+2G_\sigma(\omega)]\end{aligned}\tag{23}$$

$$\begin{aligned}&\langle\Phi_0|1/2,-\sigma\rangle\langle 0,0|\hat{c}_{k\alpha,-\sigma}|\Phi_0\rangle=-\frac{i}{2}\,F_{-\sigma}(\hat{c}_{k\alpha,-\sigma})_{t'=t}\\&=-\frac{1}{2}\int_{-\infty}^{t}d\tau\,V_{k\alpha}[F_{-\sigma}(\tau,t)-[2\langle\hat{n}_{k\alpha,-\sigma}\rangle-1]\\&\quad\times G_{-\sigma}(\tau,t)]\exp(i\epsilon_{k\alpha}(\tau-t)).\end{aligned}\tag{24}$$

2.3. General expression for the current

The current of holes from the left lead to the central region is obtained from the time evolution of the hole occupation number of the left lead (here we do not use atomic units):

$$\begin{aligned}J_L(t)&=e\,\frac{d\langle\hat{N}_L\rangle}{dt}=e\,\frac{d}{dt}\sum_{kL,\sigma}\langle\hat{c}^+_{kL,\sigma}\hat{c}_{kL,\sigma}\rangle\\&=\frac{ie}{\hbar}\sum_{kL,\sigma}\langle[H,\hat{c}^+_{kL,\sigma}\hat{c}_{kL,\sigma}]\rangle.\end{aligned}\tag{25}$$

The average values are always referred to the Φ_0 state. By solving the commutator $[H,\hat{n}_{kL,\sigma}]$ it is found that:

$$J_L(t)=-\frac{2e}{\hbar}\,\mathrm{Im}\sum_{kL,\sigma}\tilde{V}^*_{k\alpha}\langle\Phi_0|1/2,\sigma\rangle\langle 0,0|\hat{c}_{kL,\sigma}|\Phi_0\rangle\tag{26}$$

and using equation (24) we can write the following expression:

$$\begin{aligned}J_L(t)=\frac{e}{\hbar}\,\mathrm{Im}\sum_{kL,\sigma}\tilde{V}_{k\alpha}\int_{-\infty}^{t}d\tau\,\tilde{V}^*_{k\alpha}[F_\sigma(\tau,t)\\-[2\langle\hat{n}_{kL,\sigma}\rangle-1]G_\sigma(\tau,t)]\exp(i\epsilon_{kL}(\tau-t))\end{aligned}\tag{27}$$

which is equivalent to that found by Jauho *et al* [19], but expressed in terms of the Green functions $G_\sigma(\tau,t)$ and $F_\sigma(\tau,t)$ in the present case. For a time-independent process the Fourier transform of this expression is valid and we can write:

$$\begin{aligned}\frac{J_L}{(2e/h)}&=\frac{1}{2}\,\mathrm{Im}\sum_{k,\sigma}|\tilde{V}_{kL}|^2 i\\&\quad\times\int_{-\infty}^{\infty}d\omega\,\frac{F_\sigma(\omega)-[2f^{FD}(\epsilon_{kL})-1]G_\sigma(\omega)}{\omega-\epsilon_{kL}+i\eta}.\end{aligned}\tag{28}$$

Taking into account that in the steady state the current will be uniform, so that $J_R=-J_L$, the current can be symmetrized as $I=(J_L-J_R)/2$. Thus, it follows from equation (28) that:

$$\begin{aligned}\frac{I}{(2e/h)}&=\sum_\sigma\left\{\frac{1}{4}\int_{-\infty}^{\infty}d\omega\,[\Gamma^L(\omega)-\Gamma^R(\omega)]\,\mathrm{Im}[F_\sigma(\omega)\right.\\&\quad+2G_\sigma(\omega)]-\int_{-\infty}^{\infty}d\omega\,[\Gamma^L(\omega)f^{FD}(\omega-\mu_L)\\&\quad\left.-\Gamma^R(\omega)f^{FD}(\omega-\mu_R)]\,\mathrm{Im}\,G_\sigma(\omega)\right\}\end{aligned}\tag{29}$$

where $\mu_{L(R)}$ are the Fermi levels of the leads L(R)$\mu_L-\mu_R=eV$ where V is the applied bias voltage and e the elemental charge. At zero bias voltage ($\mu_L=\mu_R$), that is in equilibrium, the following identity is valid:

$$\mathrm{Im}\,F_\sigma(\omega)=2[2f^{FD}(\omega)-1]\,\mathrm{Im}\,G_\sigma(\omega)\tag{30}$$

and the current I vanishes identically.

We have introduced in equation (29) the level widths:

$$\Gamma^\alpha(\omega)=\pi\sum_k|\tilde{V}_{k\alpha}|^2\,\delta(\epsilon-\epsilon_{k\alpha}).\tag{31}$$

By using a linear expansion of the contact surface states $\phi_{k\alpha}$ in atomic orbitals φ_m centered on surface sites located at R_s positions (linear combination of atomic orbitals (LCAO) expansion), $\phi_{k\alpha}=\sum_{m,R_s}c^{k\alpha}_{m,R_s}\varphi_m(r-R_s)$, we can write that:

$$\tilde{V}_{k\alpha}=1/\sqrt{5}\sum_{d=1-5}V_{k\alpha,d}=1/\sqrt{5}\sum_{d=1-5}\sum_{m,R_s}c^{k\alpha}_{m,R_s}V^\alpha_{mR_s,d}\tag{32}$$

and therefore:

$$\begin{aligned}\Gamma^\alpha(\omega)&=\sum_{m,n,R_s,R'_s}\Gamma^\alpha_{m,n,R_s}(\omega)\\&=\pi\sum_{m,n,R_s,R'_s}V^{*\alpha}_{mR_s}V^\alpha_{nR'_s}\rho^\alpha_{m,n,R_s,R'_s}(\omega)\end{aligned}\tag{33}$$

Table 1. Coupling terms, in eV, between the central atom d-states (columns) and the states on the end atom of the left (right) lead.

$V^{\mathrm{L}}_{nR_0,\mathrm{d}}$ ($V^{\mathrm{R}}_{nR_0,\mathrm{d}}$)	d_{xy}	d_{yz}	d_{z^2}	d_{xz}	$\mathrm{d}_{x^2-y^2}$
d_{xy}	−0.010 (−0.010)	0.000 (0.000)	0.000 (0.000)	0.000 (0.000)	0.000 (0.000)
d_{yz}	0.000 (0.000)	0.075 (0.075)	0.000 (0.000)	0.000 (0.000)	0.000 (0.000)
d_{z^2}	0.000 (0.000)	0.000 (0.000)	−0.240 (−0.240)	0.000 (0.000)	0.000 (0.000)
d_{xz}	0.000 (0.000)	0.000 (0.000)	0.000 (0.000)	0.075 (0.075)	0.000 (0.000)
$\mathrm{d}_{x^2-y^2}$	0.000 (0.000)	0.000 (0.000)	0.000 (0.000)	0.000 (0.000)	−0.010 (−0.010)
s	0.000 (0.000)	0.000 (0.000)	−0.199 (−0.199)	0.000 (0.000)	0.000 (0.000)
p_x	0.000 (0.000)	0.000 (0.000)	0.000 (0.000)	0.390 (−0.390)	0.000 (0.000)
p_y	0.000 (0.000)	0.390 (−0.390)	0.000 (0.000)	0.000 (0.000)	0.000 (0.000)
p_z	0.000 (0.000)	0.000 (0.000)	−1.020 (1.020)	0.000 (0.000)	0.000 (0.000)

where now $V^{\alpha}_{nR_s} = 1/\sqrt{5}\sum_{\mathrm{d}=1-5} V^{\alpha}_{nR_s,\mathrm{d}} V^{\alpha}_{nR_s,\mathrm{d}}$ being the coupling term between a d state of the central atom and the n state of the atom positioned at R_s in lead (α), and

$$\rho^{\alpha}_{m,n,R_s,R'_s}(\epsilon) = \sum_{\mathrm{k}} c^{\mathrm{k}\alpha}_{m,R_s} c^{\mathrm{k}\alpha}_{n,R'_s} \delta(\epsilon - \epsilon_{\mathrm{k}\alpha}) \qquad (34)$$

are the density matrix elements of the corresponding (α) contact surface, being the site and orbital diagonal terms of the local and partial density of states (LDOS). We are going to consider in the calculation only the site diagonal matrix elements ($R_s = R'_s$).

The same LCAO description leading to expressions such as (33) is used for calculating the Green functions $G_\sigma(\omega)$ and $F_\sigma(\omega)$ through equations (15) and (19) respectively. In this form all our model calculation requires us to know is the electronic structure of the lead surfaces given by their density matrix elements $\rho^{\alpha}_{m,n,R_s}(\epsilon)$, the coupling $V^{\alpha}_{nR_s,\mathrm{d}}$ between the d-orbitals of the central atom and the s-, p-, d-orbitals of the atoms of the leads, and also the energy of the one hole state in the central atom. This is given by $\varepsilon_{\mathrm{d}} = (\varepsilon_{1/2} - \varepsilon_0) = [E(\mathrm{d}^9) - E(\mathrm{d}^{10})]$, with $E(\mathrm{d}^{10})$ and $E(\mathrm{d}^9)$ the total energies for the d atomic configurations with 10 (0) and 9 (1) electrons (holes) respectively.

3. Results and discussion

We considered only the interaction of the central Pd atom with the end atoms of each lead (see inset in figure 1). The distance between the central atom and the outermost atom of each lead is 3.47 bohr, this value corresponding to the equilibrium distance of a Pd trimer calculated by using the Fireball code [18]. The coupling integrals $V^{\alpha}_{nR_s,\mathrm{d}}$, corresponding to the Hamiltonian off-diagonal matrix elements in the atomic basis set, were obtained by using the same code [18]. They are shown in table 1 (in eV).

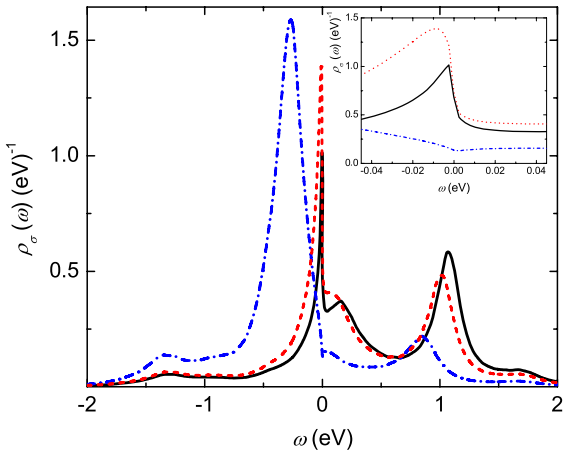

Figure 2. Projected density of states on the central atom at $T = 5$ K, and for different hole-state energies: $\varepsilon_{\mathrm{d}} = 0$ eV (dash–dot line), $\varepsilon_{\mathrm{d}} = 0.55$ eV (dashed line), and $\varepsilon_{\mathrm{d}} = 0.7$ eV (solid line). In the inset the same densities of states around the Fermi level are shown.

The value of the energy level of the central Pd atom is assumed to be close to the Fermi level of the Pd-contact surfaces. In order to analyze the sensibility to the hole energy level position, ε_{d} values going from 0 to 0.7 eV were studied finding in this reduced range of energy a change from a mixed valence to a Kondo regime.

3.1. Equilibrium: local density of states on the central Pd atom

In figure 2 one can observe the projected density of states on the Pd central atom, $\rho_\sigma(\omega)$, for $\varepsilon_{\mathrm{d}} = 0, 0.55, 0.7$ eV and at temperature $T = 5$ K. A Kondo resonance appears in the cases of $\varepsilon_{\mathrm{d}} = 0.7$ and 0.55 eV, and a mixed valence behavior corresponds to $\varepsilon_{\mathrm{d}} = 0$ eV. The presence of a dip in the density of states around the Fermi level in the case of a mixed valence

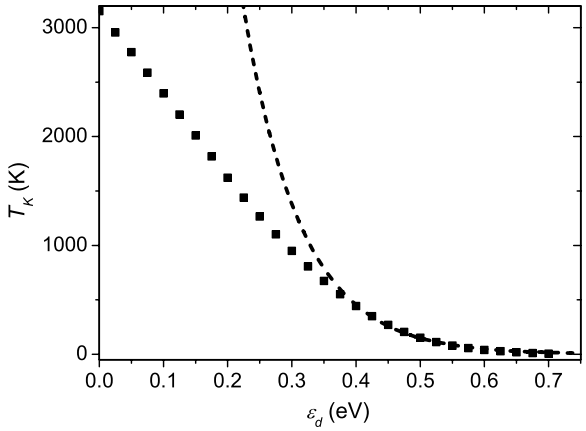

Figure 3. The Kondo temperature as a function of the hole-state energy. Full square symbols: calculated from equation (35). Dashed line: the fitting with the exponential dependence of the flat band approximation to equation (35), as it is explained in the text.

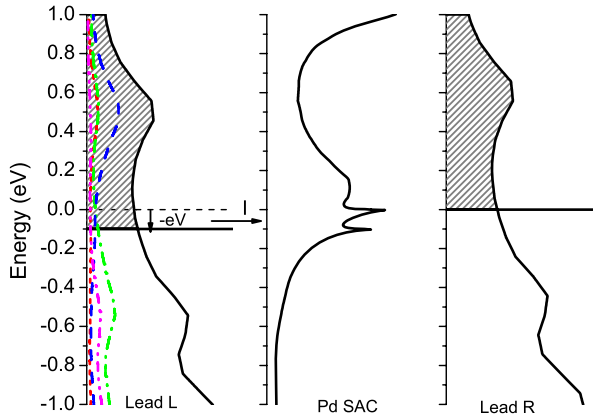

Figure 4. The LDOS on the outermost right and left contact atoms are indicated with solid lines. Dashed line: the p_z-band contribution; dashed–dotted line: $(p_x + p_y)$-band contribution; dashed–dotted–dotted line: d_{z^2}-band contribution. The dashed regions correspond to the occupied hole states, and the Fermi levels of both leads are indicated with the horizontal solid lines. The $\mathrm{Im}\, G_\sigma(\omega)/\pi$ on the Pd central atom calculated for $\varepsilon_\mathrm{d} = 0.7$ eV, $V = 0.1$ V and $T = 5$ K, is also shown.

regime is related to the second order in the V approximation used in this work [24]. The other resonance peaks appearing below and above the Fermi level, at energies around 1 eV, are introduced by the electronic structure of the two contact surfaces.

In figure 3 we show the dependence with ε_d of the temperature defined by the resonance ω_K close to 0 ($\omega_\mathrm{K} = T_\mathrm{K}/k_\mathrm{B}$) obtained from the equation:

$$\omega - \varepsilon_\mathrm{d} - \mathrm{Re}\left[\sum_{\mathrm{k}\alpha} \frac{|\tilde{V}_{\mathrm{k}\alpha}|^2}{\omega - \epsilon_{\mathrm{k}\alpha} - \mathrm{i}\eta} + \sum_{\mathrm{k}\alpha} \frac{|\tilde{V}_{\mathrm{k}\alpha}|^2 \langle \hat{n}_{\mathrm{k}\alpha,-\sigma}\rangle}{\omega - \epsilon_{\mathrm{k}\alpha} - \mathrm{i}\eta}\right] = 0. \tag{35}$$

For ε_d larger than 0.35 eV we found that our calculated values are well fitted by the expression $T_\mathrm{K} = 38\,836$ K $\times$ $\exp(-11.13\ \varepsilon_\mathrm{d})$. This exponential dependence with ε_d is the one found in the case of a flat wide band approximation of the contact surfaces, $T_\mathrm{K} = (\hat{D}/k_\mathrm{B})\exp(-\pi|\varepsilon_\mathrm{d}|/\hat{\Gamma})$, where $\hat{D}$ is the half-bandwidth of the contact surfaces and the level-width $\hat{\Gamma} = 5\Gamma_\mathrm{d}$ is defined by assuming all the $V_{\mathrm{k}\alpha,\mathrm{d}}$ (that is $\tilde{V}_{\mathrm{k}\alpha} = \sqrt{5}V_{\mathrm{k}\alpha,\mathrm{d}}$) are equal. By using the flat wide band approximation and according to the fitting parameters, we can characterize our system in the energy range $\varepsilon_\mathrm{d} > 0.35$ eV by the following effective values: $\hat{D} = 3.35$ eV and $\hat{\Gamma} = 280$ meV. The 'effective' d-level width $\Gamma_\mathrm{d} = 56$ meV is about twice as large as the typical width values obtained from measurements of the $\mathrm{d}I/\mathrm{d}V$ peak in Kondo regimes found in single-molecule transistors and controllable break junctions [15, 16, 26]. The value of $\hat{D}$ is close to the one used within our model calculation: $D = 5$ eV (see figure 1), and the 'effective' $\hat{\Gamma}$ is very similar to the level-width calculated by using equation (33) as $\Gamma = [\Gamma^\mathrm{L}(\tilde{\varepsilon}_\mathrm{d}) + \Gamma^\mathrm{R}(\tilde{\varepsilon}_\mathrm{d})] \sim 240$ meV, where $\tilde{\varepsilon}_\mathrm{d}$ is the atom energy level shifted by the interaction.

3.2. Non-equilibrium: current and conductance

The current is calculated by considering a bias voltage V applied to the left lead ($\mu_\mathrm{L} \pm eV$). The out of equilibrium Green functions $G_\sigma(\omega)$ and $F_\sigma(\omega)$ are first calculated according to expressions (15) and (19) in a consistent way with (23) and (24). Then, both these Green functions are used in equation (29) for calculating the current I. In figure 4 the case of $\mu_\mathrm{L} - eV$ is shown, and the hole current direction is indicated by taking into account the occupied hole states that correspond to the dashed regions in the LDOS of the outermost contact atoms. The $\mathrm{Im}\, G_\sigma(\omega)/\pi$ calculated in the case $\varepsilon_\mathrm{d} = 0.7$ eV and $V = 0.1$ V is also included in the same figure, showing a satellite resonance peak at energy eV [27] and the less pronounced Kondo peak due to the asymmetry created by the applied bias potential.

3.2.1. Conduction channels. Band state contributions. The current I and the respective conductance $G = \mathrm{d}I/\mathrm{d}V$ as functions of the bias voltage V are shown in figures 5(a) and (b) respectively for the case of $\varepsilon_\mathrm{d} = 0.7$ eV and for $T = 5$ K. Non-ohmic behavior of the current is observed giving place to a non-constant conductance as a function of V. By comparing the conductance versus V with the energy dependence of the LDOS on the central atom shown in figure 2, one can see that the conductance is a *register* of the LDOS shape. In figure 5 is also included the current and conductance discriminated by contact band state contributions which according to equations (29) and (33) means considering the current given by:

$$\frac{I}{(2e/h)} = \sum_{m,n} \frac{I_{m,n}}{(2e/h)}; \tag{36}$$

where the different terms related to the $m, n(=\mathrm{s, p, d})$ band states of the contact surfaces are:

$$\frac{I_{m,n}}{(2e/h)} = \sum_{\sigma,R_s}\left\{\frac{1}{4}\int_{-\infty}^{\infty}\mathrm{d}\omega\,[\Gamma^\mathrm{L}_{m,n,R_s}(\omega) - \Gamma^\mathrm{R}_{m,n,R_s}(\omega)]\,\mathrm{Im}[F_\sigma(\omega) + 2G_\sigma(\omega)]\right.$$

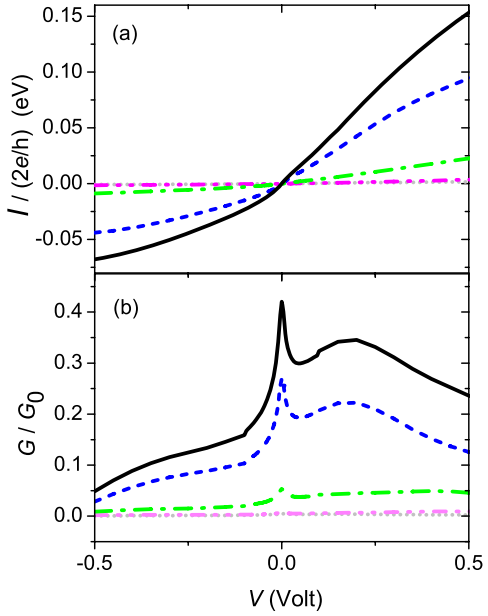

Figure 5. (a) The current as a function of the bias voltage discriminated by surface contact band contributions for $\varepsilon_{\rm d} = 0.7$ eV and $T = 5$ K; s (light gray dotted line), p_z (dashed line), d_{z^2} (dashed–dotted–dotted line), $(p_x + p_y)$ (dashed–dotted line), and the total current (solid black line). (b) The same as in (a) but for the conductance $G = {\rm d}I/{\rm d}V$.

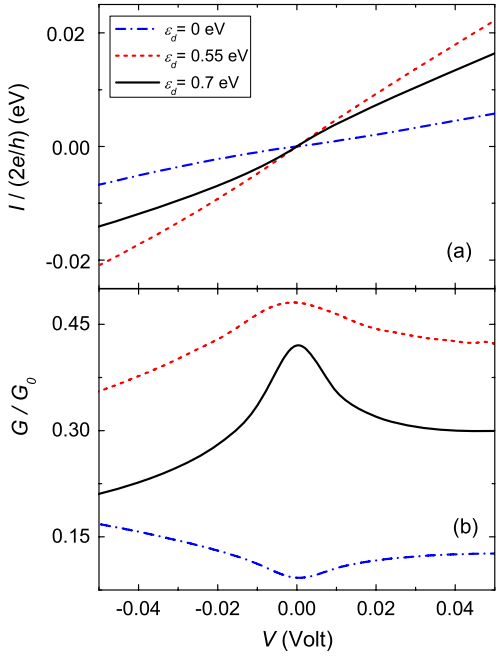

Figure 6. (a) Current and (b) differential conductance as a function of the bias voltage for $T = 5$ K and different values of the level $\varepsilon_{\rm d}$: 0.7 eV (solid line); 0.55 eV (dashed line); 0 eV (dashed–dotted line).

$$- \int_{-\infty}^{\infty} {\rm d}\omega \,[\Gamma^{\rm L}_{m,n,R_s}(\omega) f^{\rm FD}(\omega - \mu_{\rm L}) - \Gamma^{\rm R}_{m,n,R_s}(\omega) f^{\rm FD}(\omega - \mu_{\rm R})]\,{\rm Im}\, G_\sigma(\omega)\Big\}. \quad (37)$$

It is observed from figure 5 that the main contribution is provided by the $m = n = p_z$ diagonal term which corresponds to the largest width $\Gamma^{\alpha}_{p_z,p_z,R_0}(\epsilon) = \pi |V^{\alpha}_{p_z R_0}|^2 \rho^{\alpha}_{p_z,p_z R_0}(\epsilon)$ according to the values of the coupling terms $V^{\alpha}_{p_z R_0,{\rm d}}$ (see table 1) and the LDOS $\rho^{\alpha}_{p_z,p_z R_0}(\epsilon)$ shown in figure 4. By taking into account the local density of states of the leads and the values of $V^{\alpha}_{n R_0,{\rm d}}$, one can conclude that the more relevant conduction channels involve the p-band states of the contact surfaces and the d_{z^2}, d_{xz} and d_{yz} orbitals of the central atom. The same is concluded for the other $\varepsilon_{\rm d}$ cases. We have to remark that (i) the LCAO expansion of the contact surface states, (ii) the complete density matrix of the leads, and (iii) the hopping integrals, allow us to discriminate the conduction channels provided by the interplay between SAC and the lead band states.

3.2.2. Current and conductance in Kondo and mixed valence regimes. In figure 6 we show the current and conductance within a reduced range of bias voltage values (between -0.05 and 0.05 V) for the three values of $\varepsilon_{\rm d}$. The largest value of the conductance $G \sim 0.48 G_0$ for bias voltage close to 0 is found in the case of $\varepsilon_{\rm d} = 0.55$ eV. In the case $\varepsilon_{\rm d} = 0.7$ eV this value is $0.42 G_0$. While in the mixed valence regime a considerably smaller value of the conductance is found ($G \sim 0.15 G_0$).

It is interesting to analyze the two terms of expression (29) that contribute to the total current I. In figure 7 these two terms are compared for the different regimes according to the $\varepsilon_{\rm d}$ values. By a linear expansion in the bias voltage around $V = 0$, and using the identity (30), the first and second term of equation (29) can be written as:

$$[\text{first term}] \simeq -eV \times \sum_\sigma \int_{-\infty}^{\infty} {\rm d}\omega \left(\frac{\partial \Gamma^{\rm L}(\omega)}{\partial \omega} f^{\rm FD}(\omega)\, {\rm Im}\, G_\sigma(\omega) \right)_{V=0} \quad (38)$$

$$[\text{second term}] \simeq eV \times \sum_\sigma \int_{-\infty}^{\infty} {\rm d}\omega \left(\frac{\partial \Gamma^{\rm L}(\omega)}{\partial \omega} f^{\rm FD}(\omega)\, {\rm Im}\, G_\sigma(\omega) \right)_{V=0} + eV \sum_\sigma \int_{-\infty}^{\infty} {\rm d}\omega \left(\Gamma^{\rm L}(\omega) \frac{\partial f^{\rm FD}}{\partial \omega}\, {\rm Im}\, G_\sigma(\omega) \right)_{V=0}. \quad (39)$$

The first one takes into account the energy dependence of the LDOS of both leads. The second term, equation (39), has a contribution proportional to the LDOS around the Fermi level in the case of low temperatures, and another one which is equal to minus the only contribution to the first term (equation (38)). This fact explains the negative conductance values found in the case of the second term (figure 7(d)), and allows us to arrive at the following expression of the conductance for zero bias potential:

$$\frac{G\,(T, V = 0)}{G_0} = \sum_\sigma \int_{-\infty}^{\infty} {\rm d}\omega \left(\Gamma^{\rm L}(\omega) \frac{\partial f^{\rm FD}}{\partial \omega}\, {\rm Im}\, G_\sigma(\omega) \right)_{V=0} \quad (40)$$

that gives $G/G_0 = 2\pi\ \Gamma^{\rm L}(0)\ \rho_\sigma(0)$ at $T = 0$ K.

3.2.3. Temperature behavior of the conductance. The temperature behaviors of the density of states $\rho_\sigma(\omega)$ and of the

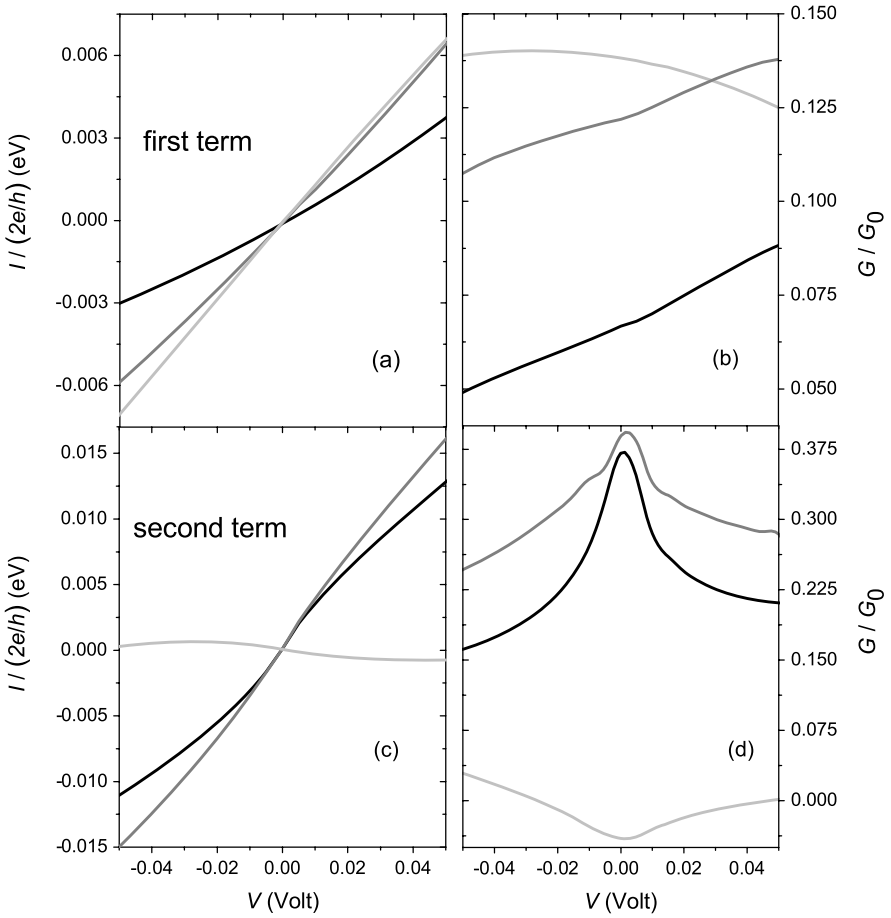

Figure 7. The contribution of the first term given by equation (38) to the current (a) and to the differential conductance (b) as a function of the bias voltage for $T = 5$ K and for the different values of ε_d. The contribution of the second term given by equation (39) to the current and differential conductance is shown in (c) and (d) respectively. Solid black line: $\varepsilon_d = 0.7$ eV; gray solid line: $\varepsilon_d = 0.55$ eV; light gray solid line: $\varepsilon_d = 0$ eV.

zero bias voltage conductance obtained in the Kondo regime for $\varepsilon_d = 0.7$ eV are shown in figure 8 within a temperature range from 5 to 600 K. The calculated temperature dependence of the zero bias voltage conductance (figure 8(c)) can be well fitted by the expression:

$$\frac{G(T, V = 0)}{G_0} = \tilde{G}_0 \left[1 + \frac{T^2}{\tilde{T}_K^2} (2^{1/s} - 1) \right]^{-s} + G_e \qquad (41)$$

using $\tilde{G}_0$, $\tilde{T}_K$, and G_e as fitting parameters and $s = 0.22$. Expression (41) with $s = 0.22$ matches the slope of the conductance fall-off found in numerical renormalization group calculations for spin-1/2 Kondo systems [28]; therefore we can conclude that our calculated conductance values follow the same behavior with the temperature predicted by the exact calculation. The temperature-independent offset G_e added to the Kondo form [29] accounts for non-Kondo conduction channels present at temperatures above $\tilde{T}_K$ [30]. In our case we found from equation (41) $\tilde{T}_K \simeq 212$ K, a value in good agreement with the corresponding temperatures around 200 K calculated by considering $k_B T_K \sim$ FWHM (full width at half maximum) of the Kondo resonance peak of the LDOS (figure 8(a)) or $k_B T_K/e \sim$ FWHM of the zero bias conductance peak (figure 8(b)) at $T \sim 0$ K [15]. A Pd SAC constructed with these features corresponds to a Kondo regime with a widened resonance Kondo peak, then the temperatures associated with either its width or with the resonance energy position differ greatly (see figure 3). On the other hand, the $\tilde{T}_K$ value we obtained from the temperature dependence of the zero bias voltage conductance is between five and ten times larger than the corresponding values obtained from measurements of the dI/dV peak in Kondo regimes found in several nanodevices [15, 16, 26].

The temperature dependence of the conductance $G(T, V = 0)$ found in the cases of $\varepsilon_d = 0.55$ and 0 eV can be seen in figure 9. In the $\varepsilon_d = 0.55$ eV case an increase with the temperature conductance below $T \simeq 30$ K is observed where G gets its maximum value of $0.5G_0$. For $T > 30$ K the conductance diminishes, reaching a value of $0.4G_0$ at room temperature. The temperature dependence of the conductance does not follow equation (41) in these ε_d cases. In the mixed valence regime the conductance grows as temperature is increased, being $G = 0.15G_0$ at room temperature. In this regime the dip observed in the conductance (or in the LDOS) at the Fermi energy disappears at temperatures higher than 200 K, and a smoother behavior is recovered [24].

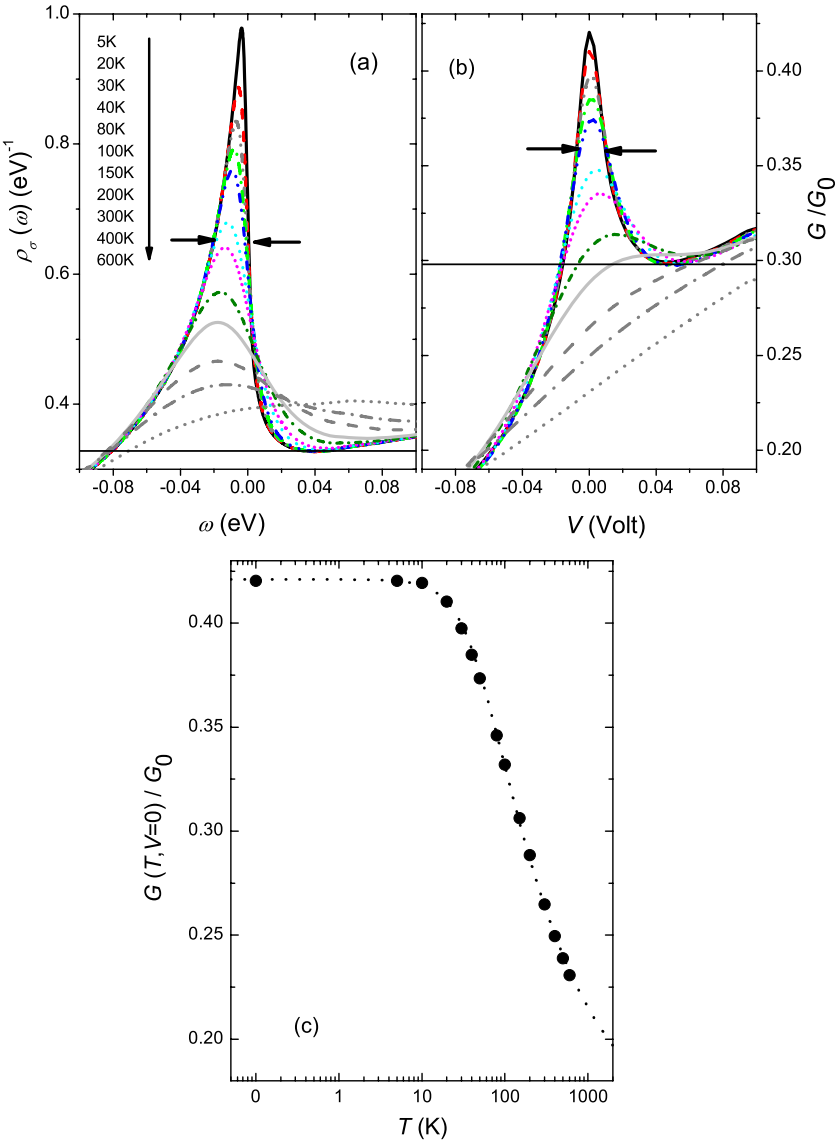

Figure 8. In the Kondo regime ($\varepsilon_d = 0.7$ eV): (a) the local density of states on the central atom, close to the Fermi level and for several temperatures; (b) the differential conductance as a function of the bias voltage for the same temperature values as in (a); (c) temperature dependence of the zero bias conductance (full circle); the dotted line is the fitting with equation (41).

4. Conclusions

The conduction through a Pd SAC between two pyramidal structured contact surfaces of pure Pd is analyzed by assuming the d^{10} to d^9 charge fluctuation as the most probable one in the single atom. This means a total spin fluctuation between $S = 0$ and $1/2$ within the more appropriate hole description. Five-fold d-orbital degeneration is considered and the EOM method closed up to a second order in the coupling parameter is employed to solve the electronic transport characteristics. Small variations of the Pd atom energy level position change the correlated regime from a Kondo to a mixed valence one. The Kondo regime found in our system is characterized by a level-width and a Kondo temperature that are between five and ten times larger than the corresponding values estimated in Kondo regimes observed in mechanically controllable break junction experiments and single-molecule transistors [26, 15, 16]. We calculated conductance values less than G_0 in agreement with measured values in these kinds of experiments, and also with the reported conductance values of Rodrigues *et al* [5] in Pd break junctions. The calculated conductance at zero bias voltage in the Kondo regime falls with increasing temperature with the slope found in numerical renormalization group calculations for spin-1/2 Kondo systems.

As previous theoretical results have shown [31], the conductance of a small contact depends on the geometrical and electronic configuration of the neck formed around the center of the contact. In this sense our model calculation is highly promising because it allows us to include all the features of the interacting systems through the LDOS of the contact surfaces, the atom–atom coupling integrals, and the atom energy levels involved. Within a general treatment of processes out of equilibrium and choosing the conduction

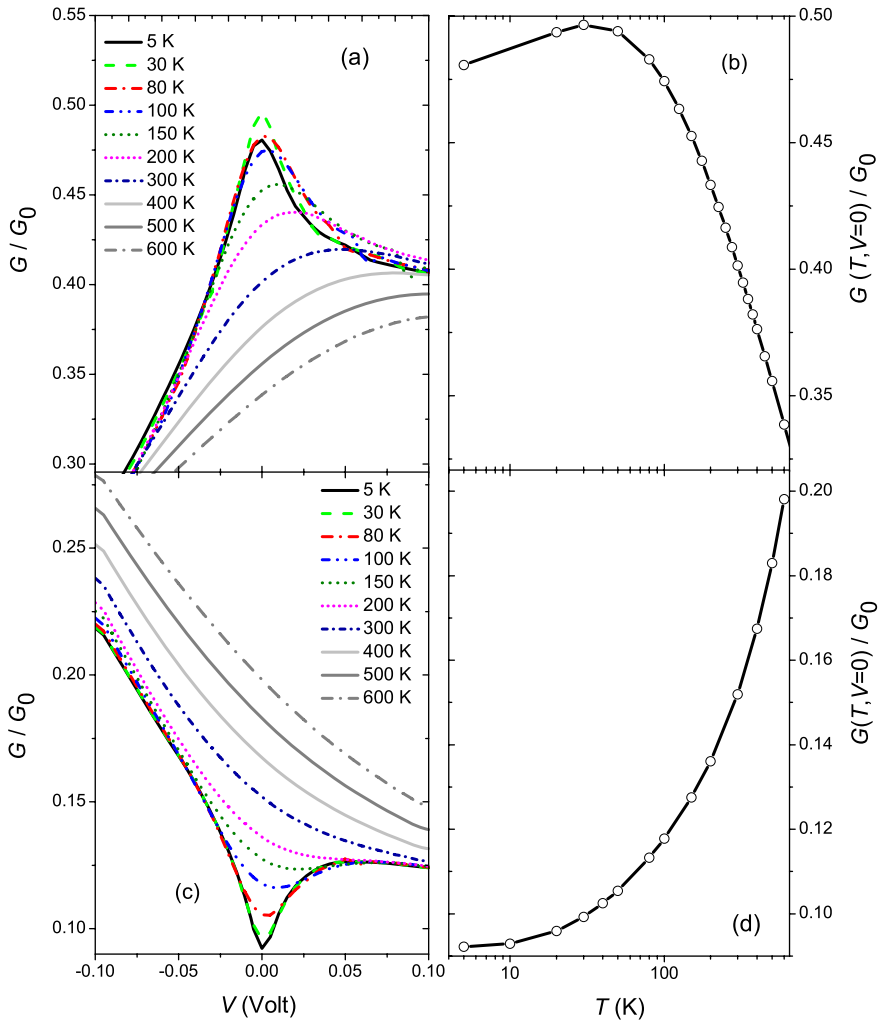

Figure 9. (a) Conductance versus bias voltage for several temperatures and (b) zero bias conductance as a function of temperature for $\varepsilon_d = 0.55$ eV. (c) and (d): the same as (a) and (b) for $\varepsilon_d = 0$ eV.

channels associated with the possible charge fluctuations in the SAC, the contributions of the different atoms and band states of the contact surfaces can be straightforwardly calculated.

In summary, in this work we included the extended properties of the leads and the local ones of the central atom in the description of the nanodevices. The formalism we proposed is able to incorporate all these properties in the current calculation, and it also allows us to select the localized *dot* electronic configurations that are most probable from an energetic point of view.

Acknowledgments

The authors acknowledge financial support from CONICET. This work was supported by ANPCyT through PICT 14724 and PICT 11769, Fundación Antorchas (14248-128), CONICET through PIP 5277, and UNL through CAI+D grants. We gratefully acknowledge Fernando Flores for fruitful discussions.

References

[1] Agrait N, Levy Yeyati A and van Ruitenbeek J 2003 *Phys. Rep.* **377** 81
[2] Elhoussine F, Matefi-Tempfli S, Encinas A and Piraux L 2002 *Appl. Phys. Lett.* **81** 1681
[3] Shimizu M, Saitoh E, Miyajima H and Otani Y 2002 *J. Magn. Magn. Mater.* **239** 243
[4] Gillingham D, Linington I, Müller C and Bland J 2003 *J. Appl. Phys.* **93** 7388
[5] Rodrigues V, Bettini J, Silva P and Ugarte D 2003 *Phys. Rev. Lett.* **91** 096801
[6] Csonka Sz, Halbritter A and Mihaly G 2004 *Phys. Rev. Lett.* **93** 016802
[7] Li J, Kanzaki T, Murakoshi K and Nakato Y 2002 *Appl. Phys. Lett.* **81** 123
[8] Untiedt C, Dekker D M, Djukic D and van Ruitenbeek J M 2004 *Phys. Rev.* B **69** 081401
[9] Scheer E, Agrait N, Cuevas J, Levy-Yeyati A, Ludoph B, Martín-Rodero A, Rubio Bollinger G, van Ruitenbeek J and Urbina C 1998 *Nature* **394** 154
[10] Scheer E, Joyez P, Esteve D, Urbina C and Devoret M 1997 *Phys. Rev. Lett.* **78** 3535
[11] Cuevas J, Levy-Yeyati A, Martín-Rodero A, Rubio Bollinger G, Untiedt C and Agrait N 1998 *Phys. Rev. Lett.* **81** 2990

[12] Smit R H M, Untiedt C, Yanson A I and van Ruitenbeek J M 2001 *Phys. Rev. Lett.* **87** 266102
[13] Jamneala T, Madhavan V, Chen W and Crommie M F 2000 *Phys. Rev.* B **61** 9990
[14] Neel N, Kroger J, Limot L, Palotas K, Hofer W A and Berndt R 2007 *Phys. Rev. Lett.* **98** 016801
[15] Liang W, Shores M P, Bockrath M, Long J R and Park H 2002 *Nature* **417** 725
Park H, Pasupathy A N, Goldsmith J I, Chang C, Yaish Y, Petta J R, Rinkoski M, Sethna J P, Abruña H D, McEuen P L and Ralph D C 2002 *Nature* **417** 722
[16] Yu L H, Keane Z K, Ciszek J W, Cheng L, Tour J M, Baruah T, Pederson M R and Natelson D 2005 *Phys. Rev. Lett.* **95** 256803
[17] Keldysh L V 1964 *Zh. Eksp. Teor. Fiz.* **47** 1515
Keldysh L V 1965 *Sov. Phys.—JETP* **20** 1018 (Engl. Transl.)
[18] FIREBALL
Sankey O F and Niklewski D J 1989 *Phys. Rev.* B **40** 3979
Demkov A A *et al* 1995 *Phys. Rev.* B **52** 1618
[19] Jauho A-P, Wingreen N S and Meir Y 1994 *Phys. Rev.* B **50** 5528
[20] Hewson A C 1993 *The Kondo Problem to Heavy Fermions* (Cambridge: Cambridge University Press)
[21] Goldberg E C, Flores F and Monreal R 2005 *Phys. Rev.* B **71** 035112
[22] Goldberg E C and Flores F 2008 *Phys. Rev.* B **77** 125121
[23] Lacroix C 1981 *J. Phys. F: Met. Phys.* **11** 2389
[24] Monreal R and Flores F 2005 *Phys. Rev.* B **72** 195105
[25] Meir Y, Wingreen N S and Lee P A 1991 *Phys. Rev. Lett.* **66** 3048
Meir Y, Wingreen N S and Lee P A 1993 *Phys. Rev. Lett.* **70** 2601
[26] Parks J J, Champagne A R, Hutchison G R, Flores-Torres S, Abruña H D and Ralph D C 2007 *Phys. Rev. Lett.* **99** 026601
[27] Wang R, Zhou Y, Wang B and Xing D Y 2007 *Phys. Rev.* B **75** 045318
[28] Costi T A, Hewson A C and Zlatic V 1994 *J. Phys.: Condens. Matter* **6** 2519
[29] Goldhaber-Gordon D, Shtrikman H, Mahalu D, Abusch-Magder D, Meirav U and Kastner M A 1998 *Nature* **391** 156
[30] Pustilnik M and Glazman L 2001 *Phys. Rev. Lett.* **87** 216601
[31] Sirvent C, Rodrigo J G, Vieira S, Jurczyszyn L, Mingo N and Flores F 1996 *Phys. Rev.* B **53** 16086